Generating Programmatic Referring Expressions via Program Synthesis

Jiani Huang [1] **Calvin Smith** [2] **Osbert Bastani** [1] **Rishabh Singh** [3] **Aws Albarghouthi** [2] **Mayur Naik** [1]

Abstract

Incorporating symbolic reasoning into machine learning algorithms is a promising approach to improve performance on learning tasks that require logical reasoning. We study the problem of generating a programmatic variant of *referring expressions* that we call referring relational programs. In particular, given a symbolic representation of an image and a target object in that image, the goal is to generate a relational program that uniquely identifies the target object in terms of its attributes and its relations to other objects in the image. We propose a neurosymbolic program synthesis algorithm that combines a policy neural network with enumerative search to generate such relational programs. The policy neural network employs a program interpreter that provides immediate feedback on the consequences of the decisions made by the policy, and also takes into account the uncertainty in the symbolic representation of the image. We evaluate our algorithm on challenging benchmarks based on the CLEVR dataset, and demonstrate that our approach significantly outperforms several baselines.

1. Introduction

Incorporating symbolic reasoning with deep neural networks (DNNs) is an important challenge in machine learning. Intuitively, DNNs are promising techniques for processing perceptual information; then, symbolic reasoning should be able to operate over the outputs of the DNNs to accomplish more abstract tasks. Recent work has successfully applied this approach to question-answering tasks, showing that leveraging programmatic representations can substantially improve performance—in particular, in visual question answering, by building a programmatic representation of the question and a symbolic representation of the image, we can evaluate the question representation in the context of the image representation to compute the answer (Yi et al., 2018; Mao et al., 2019; Ma et al., 2019).

A natural question is whether incorporating symbolic reasoning with DNNs can be useful for tasks beyond question answering. In particular, consider the problem of generating a *referring expression*—i.e., an image caption that uniquely identifies a given *target object* in a given image (Golland et al., 2010; Kazemzadeh et al., 2014). In contrast to visual question answering, where we translate a question to a program and then execute that program, in this case, we want to *synthesize* a program identifying the target object and then translate this program into a caption.

In this paper, we take a first step towards realizing this approach. In particular, we study the problem of generating a programmatic variant of referring expressions that we call *referring relational programs*. We assume we are given a symbolic representation of an image—such a representation can be constructed using state-of-the-art deep learning algorithms (Redmon et al., 2016; Krishna et al., 2017; Yi et al., 2018; Mao et al., 2019)—together with a target object in that image. Then, our goal is to synthesize a relational program that uniquely identifies the target object in terms of its attributes and its relations to other objects in the image. Figure 1 (left) shows an example of an image from the CLEVR dataset, and two referring relational programs for object G in this image. The task for this image is challenging since G has identical attributes as H, which means that the program must use spatial relationships to distinguish them.

Our formulation of referring relational programs can take into account the uncertainty in the predictions of the DNN used to construct the symbolic representation of the image. One approach would be to use probabilistic reasoning, but doing so can be computationally intractable. Instead, we use an approach based on uncertainty sets—we construct uncertainty sets that include all DNN predictions above a certain probability threshold, and require that the referring relational program uniquely identify the target object for *all* possible configurations in these uncertainty sets.

Based on this formulation, we propose an algorithm for synthesizing referring relational programs given the sym-

[1]University of Pennsylvania [2]University of Wisconsin-Madison [3]Google Brain. Correspondence to: Jiani Huang <jianih@seas.upenn.edu>.

Proceedings of the 37^{th} International Conference on Machine Learning, Vienna, Austria, PMLR 119, 2020.

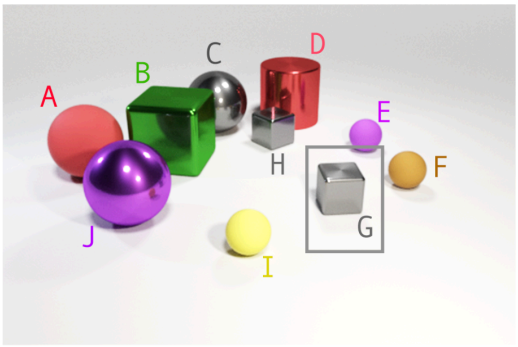

Program 1:

```
color(var0, gray)
/\ front(var0, var1)
/\ color(var1, brown)
```

Output:

{ var0 = **G**, var1 = **F** }

Program 2:

```
color(var0, gray)
/\ front(var0, var1)
/\ shape(var1, cube)
```

Output:

{ var0 = **G**, var1 = **C** }
{ var0 = **G**, var1 = **B** }

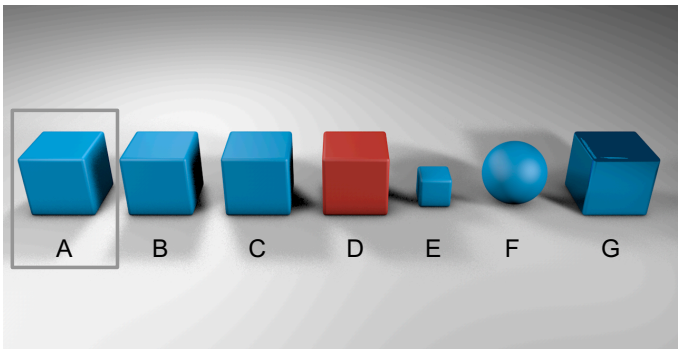

Program:

```
color(var0, blue) /\ shape(var0, cube) /\ size(var0, large)
/\ left(var0, var1) /\ left(var1, var2)
/\ left(var0, var2) /\ color(var2, blue) /\ shape(var2, cube)
/\ size(var2, large) /\ material(var2, rubber)
```

Output:

{ var0 = **A**, var1 = **B**, var2 = **C** }

Figure 1. Left: An example image from the CLEVR dataset, and two referring relational programs that identify the target object G. The challenge is distinguishing G from the second gray cube H. The first program identifies the target object as the "gray object in front of the brown object", where the brown object is the sphere F. The second program identifies the target object as the "gray object in front of the cube". In this case, the cube can be either B or H, but either of these choices uniquely identifies G. Right: A challenging problem instance that requires several relations to solve (especially when restricted to three free variables—i.e., $|\mathcal{Z}| = 3$). The program shown is generated by our algorithm. It identifies the target object as "the large blue cube to the left of the object to the left of a large blue rubber cube".

bolic representation of the image.[1] Fundamentally, program synthesis is a combinatorial search problem. The objective is to search over the space of possible programs to find one that achieves the given goal—in our case, find a relational program that uniquely identifies the target object when evaluated against the symbolic representation of the image.

To account for the combinatorial size of the search space, our synthesis algorithm builds on recent techniques for speeding up program synthesis. First, it leverages *execution-guided synthesis* (Chen et al., 2018), where deep learning is used to guide the search over the space of programs. This approach formulates the search problem as a Markov decision process, where actions correspond to decisions about which statements to include in the program, and states correspond to the intermediate program state obtained by incrementally evaluating the program generated so far. Then, it uses deep reinforcement learning to solve the synthesis problem. In particular, we use deep Q-learning, where the Q-network is a graph convolutional network (GCN) that takes as input a graph encoding of the program state; then, the Q-value for each action is evaluated based on local representations, avoiding the use of a lossy global representation.

Second, we leverage *hierarchical synthesis* (Nye et al., 2019), where the neurosymbolic synthesizer is combined with a faster but unguided enumerative synthesizer—intuitively, the neurosymbolic synthesizer generates the majority of the program. Then, the enumerative synthesizer fills in the remainder of the program, which tends to be a smaller but more challenging search problem. Finally, we use a simple *meta-learning* approach (Si et al., 2018b), where the Q-network is pretrained on a benchmark of training synthesis tasks; this Q-network is used to initialize the Q-networks for solving future synthesis tasks.

We evaluate our approach on the CLEVR dataset (Johnson et al., 2017), a synthetic dataset of objects with different attributes and spatial relationships. Our goal is to generate a relational program that identifies one of the objects in the scene. We consider both synthetic examples where the ground truth scene graph is known, as well as cases where the scene graph is predicted using a convolutional neural network (CNN) and may be prone to error. We leverage control over the data generation process to generate problem instances that are particularly challenging—i.e., where there are multiple objects with the same attributes in each scene. By doing so, a valid relational referring program must include complex spatial relationships to successfully identify the target object. We demonstrate how our approach outperforms several baselines, including a state-of-the-art program synthesizer (Si et al., 2018b).

Finally, we discuss how our approach connects to the original referring expressions task in Section 5.

Related work. There has been a great deal of recent interest in leveraging program synthesis to improve machine learning—e.g., to classify images based on their parts (Lake et al., 2015), to infer the structure of images (Ellis et al., 2015; 2018b; Pu et al., 2018), to perform procedural tasks

[1]Our implementation is available at: https://github.com/moqingyan/object_reference_synthesis.

over images (Gaunt et al., 2017; Valkov et al., 2018), to generate images with programmatic structure (Young et al., 2019), and interpretable and robust reinforcement learning (Verma et al., 2018; Bastani et al., 2018; Verma et al., 2019; Jothimurugan et al., 2019; Inala et al., 2020). These techniques demonstrate how incorporating program synthesis into machine learning tasks can improve performance on tasks that involve programmatic or symbolic reasoning.

Most closely related, there has been interest in leveraging programmatic reasoning in the domain of visual question answering (Mao et al., 2019; Ma et al., 2019). These approaches translate the question into a program using semantic parsing, and translate the image into a symbolic representation (e.g., a scene graph encoding the object attributes and relationships); then, they execute the program in the context of the symbolic representation as input to produce the answer to the given question.

Whereas visual question answering corresponds to *executing* a program in the context of the scene graph, our key insight is that generating a referring expression corresponds to *synthesizing* a program that, when executed in the context of the scene graph, produces the given target object. Recent approaches have used deep learning to generate referring expressions (Yu et al., 2016)—e.g., by leveraging a learned comprehension module (Yu et al., 2017; Luo & Shakhnarovich, 2017) or neural module networks (Liu et al., 2019). Unlike our approach, these ones do not incorporate programs and their semantics into the learning algorithm.

There has been work on incorporating logical reasoning into deep neural networks to perform reasoning tasks such as sorting and shortest path (Dong et al., 2019) or solving Sudoku problems (Wang et al., 2019), including work incorporating relational reasoning into deep neural networks to improve question answering (Santoro et al., 2017) and planning (Santoro et al., 2018), as well as general frameworks incorporating relational programs with probabilistic inference (De Raedt et al., 2007) or deep learning (Cohen et al., 2018; Manhaeve et al., 2018). In contrast, our goal is to *generate* relational programs to achieve some goal.

There has been work on synthesizing relational programs (Albarghouthi et al., 2017; Si et al., 2018a; Raghothaman et al., 2019; Si et al., 2019), though this work focuses on relational programs with different structure than ours. In particular, they typically assume the space of possible rules is not too large, and the goal is to find the right combination of rules; in contrast, our goal is to find a single rule in a combinatorially large search space of rules. There has also been work on using machine learning to speed up synthesis (Menon et al., 2013; Balog et al., 2017; Parisotto et al., 2017; Bunel et al., 2018; Feng et al., 2018; Ellis et al., 2018a); which we leverage in our algorithm.

2. Referring Relational Programs

Scene graph representation of images. We represent images via *scene graphs* $G \in \mathcal{G}$. Vertices in G are objects in the image, and edges encode relations between objects. Unary relations represent attributes such as color and shape, and binary relations capture spatial information between objects—above, left, right, and the like. Abstractly, we think of G as a set of relations over objects:

$$G = \left\{\rho_i(o_1^i, \ldots, o_{n_i}^i)\right\}_{i=1}^{n},$$

where $\rho_i \in \mathcal{R}$. Relations $\rho(o_1, ..., o_n)$ can be certain, uncertain, or absent. Certain are guaranteed to be in the graph, absent relations are guaranteed to not be in the graph, and uncertain relations may or may not be in the graph. We represent this decomposition by writing $G = G_+ \sqcup G_?$ as the *disjoint union* of the certain relations G_+ and the uncertain relations $G_?$; absent relations are omitted.

Relational programs. Our search space consists of *relational programs*, which we view as sets of relations over variables. More precisely, let $\mathcal{Z}$ be a finite set of variables, with $z_t \in \mathcal{Z}$ a *target variable* representing the object being referred to. A relational program has the form:

$$P = \bigwedge_{i=1}^{m} \rho_i(z_1^i, ..., z_{n_i}^i).$$

A *valuation* $v \in \mathcal{V}$ is a function $v : \mathcal{Z} \to \mathcal{O}$ that maps each variable to an object in the scene. Given a valuation, we can *ground* the variables in a program using $[\![\cdot]\!]$: [2]

$$[\![P]\!]_v = \bigwedge_{i=1}^{m} \rho_i(v(z_1^i), ..., v(z_{n_i}^i))$$

We will equivalently interpret $[\![P]\!]_v$ as the set of concrete relationships in the conjunction—i.e.,

$$[\![P]\!]_v = \left\{\rho_i(v(z_1^i), ..., v(z_{n_i}^i))\right\}_{i=1}^{m}$$

In this case, the grounding $[\![\cdot]\!]$ converts P into a set of predicates over objects. Then we can treat $[\![P]\!]_v : \mathcal{G} \to \mathbb{B}$, where $\mathbb{B} = \{\text{true}, \text{false}\}$, as a Boolean function over scene graphs defined so that $[\![P]\!]_v(G) = ([\![P]\!]_v \subseteq G)$—i.e., $[\![P]\!]_v(G)$ is true if and only if all of the relationships in $[\![P]\!]_v$ are also contained in G.

Definition 2.1 A valuation $v \in \mathcal{V}$ is *valid* for relational program P and scene graph G iff $[\![P]\!]_v(G) = \text{true}$.

We denote the set of all valid valuations for P in G by

$$[\![P]\!]_G = \{v \in \mathcal{V} \mid [\![P]\!]_v(G)\}.$$

[2] We use the notation $[\![P]\!]_v$ to denote the *semantics* of a program P—i.e., the output obtained by evaluating P. In our case, P evaluates into a logical formula over objects, which can be interpretered as a function mapping scene graphs to true/false.

Algorithm 1 Our algorithm for synthesizing referring relational programs. Hyperparameters are $N, M, K \in \mathbb{N}$.

function SynthesizeProgram(G)
  Initialize Q-network Q_θ with pretrained parameters θ^0
  for $i \in \{1, ..., N\}$ **do**
    Sample program P of length M according to Q_θ
    if $\phi_G(P)$ **then**
      return P
    Update Q_θ using deep Q learning
  Get best length $M - K$ program P^0 according to Q_θ
  for Programs P of length K **do**
    if $\phi_G(P^0 \wedge P)$ **then**
      return $P^0 \wedge P$
  return $\varnothing$

Referring relational programs. Our goal is to generate a relational program that satisfies the properties of a referring expression (Golland et al., 2010; Kazemzadeh et al., 2014). Given a scene and an object o_t in that scene, a referring expression is a natural language caption that uniquely identifies o_t. Figure 1 shows an example of an image together with referring relational programs that identify the target object in that image, and Figure 2 shows an example of a scene graph (ignoring the gray variable nodes).

We study a *symbolic variant* of this problem—i.e., (i) we assume the image is given as a scene graph G (e.g., these can be constructed using deep learning (Redmon et al., 2016; Krishna et al., 2017; Yi et al., 2018; Mao et al., 2019)), and (ii) our referring expressions are relational programs that uniquely identify o_t. More precisely, given a scene graph G and an object o_t in G, we want to construct a relational program P such that z_t *must* refer to o_t in the context of G.

Definition 2.2 Given scene graph G and target object o_t in G, P is a *referring relational program* for o_t in G if (i) $[\![P]\!]_{G_+} \neq \varnothing$, and (ii) for all $v \in [\![P]\!]_G$, $v(z_t) = o_t$.

Intuitively, a referring relational program must (i) have at least one certain interpretation, and (ii) all interpretations must refer to the target object, *regardless of the value of uncertain relations*. In the rest of this paper, we assume o_t is encoded in G via a unary *target* relation, and use the predicate $\phi_G(P)$ to indicate P is a referring relational program for the encoded o_t in G.

3. Program Synthesis Algorithm

Next, we describe our algorithm that, given a scene graph G, synthesizes a referring relational program P for G. At a high level, we formulate the synthesis problem as a Markov decision process (MDP). We then use reinforcement learning to learn a good policy π for this MDP on a training benchmark. Then, given a new test graph G, we continue to fine-tune π holding G fixed, and return once we find a referring relational program P for G. Our algorithm is summarized in Algorithm 1.

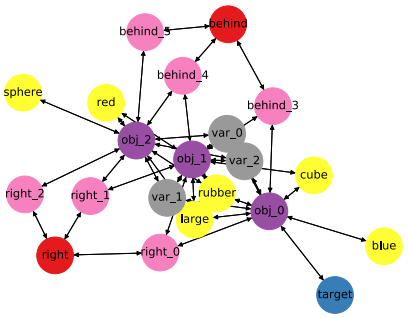

Figure 2. Example of a graph encoding of a state. Variables are shown in gray and objects are shown in purple. Binary relationships are shown in red (for a vertex ρ) and pink (for a vertex (i, ρ_i)). Unary relationships are shown in yellow; these relationships only have a single object, so we do not need a separate vertex for each relationship in (i, ρ_i). The target relationship is shown in blue.

Formulation as an MDP. We begin by describing how to formulate the problem of synthesizing a referring relational program as a Markov decision process (MDP); Figure 3 visualizes our MDP. Intuitively, since we want the MDP to encode a search over relational programs, one approach would be to choose the states to be relational programs P and the actions to be predicates $\rho(z_1, ..., z_n)$; then, taking such an action in state P transitions the system to

$$P' = P \wedge \rho(z_1, ..., z_n)$$

While this approach is possible, the states are not very informative since they do not encode any information about the semantics of relational programs. Intuitively, a policy for this MDP would have to internally construct an interpreter for relational programs to achieve good performance.

Instead, we build on an approach known as *execution-guided synthesis* (Chen et al., 2018), where the states are the outputs produced by executing programs P. Intuitively, our goal is to compute a program P such that all consistent valuations uniquely identify the target object—i.e., $v(z_t) = o_t$. Thus, given a graph $G \in \mathcal{G}$ for the current image (which is fixed for a rollout), we consider the output of P to be the set of valuations $v \in \mathcal{V}$ that are consistent with G.

In particular, the states $s \in S$ in our MDP are $s = (G, V)$, where G is a scene graph and $V \subseteq \mathcal{V}$ is a subset of valuations. Given a graph G, the initial state is $s_0 = (G, \mathcal{V})$; this choice corresponds to the empty program $P_0 = \text{true}$ (so $[\![P_0]\!]_G = \mathcal{V}$). Next, the actions $a \in A$ in our MDP are

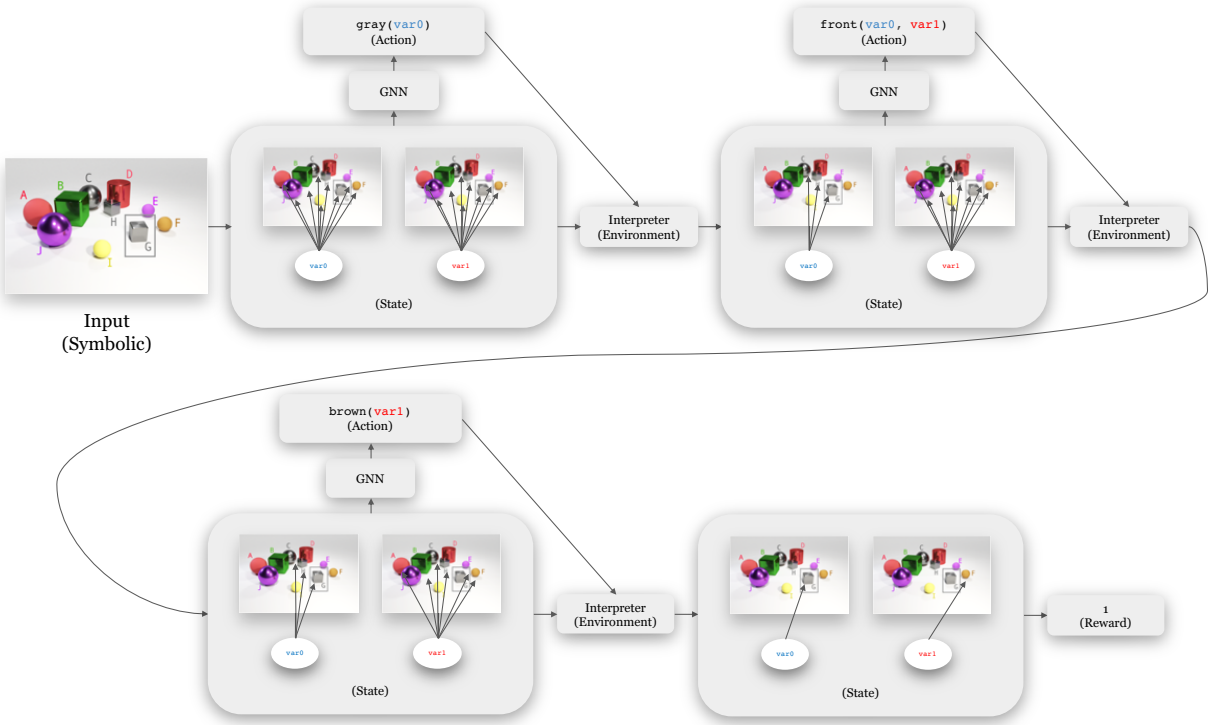

Figure 3. Example rollout according to our MDP. The input is a symbolic representation of the image as a graph. The states encode possible assignments of variables to objects in the scene; these are represented as graphs such as the one shown in Figure 2. The actions are clauses $\rho(z_1, ..., z_n)$; an action is chosen according to the Q-values predicted by the GNN Q-network. The interpreter, which serves as the "environment", removes the variables assignments that are no longer permitted by the newly chosen clause.

$a = (\rho, z_1, ..., z_n) \in \mathcal{R} \times \mathcal{Z}^*$,

$$(G, V') = T((G, V), (\rho, z_1, ..., z_n))$$
$$V' = \{v \in V \mid [\![\rho(z_1, ..., z_n)]\!]_v(G)\}.$$

That is, V' is the set of all valuations that are consistent with G given the additional predicate $\rho(z_1, ..., z_n)$. Finally, we use a sparse reward function

$$R((G, V)) = \mathbb{1}(\forall v \in V.\ v(z_t) = o_t).$$

In particular, suppose we take a sequence of actions

$$(\rho_1, z_1^1, ..., z_{n_1}^1), ..., (\rho_m, z_1^m, ..., z_{n_m}^m).$$

Then, letting P be the relational program

$$P = \bigwedge_{i=1}^{m} \rho_i(z_1^i, ..., z_{n_m}^i),$$

the state V after taking these actions equals is

$$V = \{v \in \mathcal{V} \mid [\![P]\!]_v(G)\} = [\![P]\!]_G.$$

Thus, $R((G, V)) = 1$ if and only if the program P corresponding to the sequence of actions taken is a referring relational program for G. Thus, a policy that achieves good reward on this MDP should quickly identify a valid referring relational program for a given graph G.

To handle uncertain relationships, we keep track of both certain and uncertain relationships—i.e., the initial state is $s_0 = (G, \mathcal{V}, \varnothing)$, and the transitions are

$$(G, V'_+, V'_?) = T((G, V), (\rho, z_1, ..., z_n))$$

where

$$V'_+ = \{v \in V_+ \mid [\![\rho(z_1, ..., z_n)]\!]_v(G_+)\}$$
$$V'_? = \{v \in V_? \mid [\![\rho(z_1, ..., z_n)]\!]_v(G)\}$$
$$\cup \{v \in V_+ \mid [\![\rho(z_1, ..., z_n)]\!]_v(G_?)\}.$$

Finally, the rewards are as before—i.e.,

$$R((G, V_+, V_?)) = \mathbb{1}(\forall v \in V_+ \cup V_?.\ v(z_t) = o_t)$$

Reinforcement learning. We use the deep Q-learning algorithm with a replay buffer to perform reinforcement learning—surprisingly, we found this approach outperformed policy gradient and actor-critic approaches. Intuitively, we believe it works well since the states in our formulation capture a lot of information about the progress of the

policy. Given the deep Q-network $Q_\theta(s, a)$, the corresponding policy π is to use $Q_\theta(s, a)$ with ϵ-greedy exploration—i.e., $\pi(s) = \arg\max_{a \in A} Q_\theta(s, a)$ with probability $1 - \epsilon$, and $\pi(s) \sim \text{Uniform}(A)$ with probability ϵ.

State encoding. A key challenge is designing a neural network architecture for predicting $Q_\theta(s, a)$. Our approach is based on encoding $s = (G, V)$ as a graph data structure, and then choosing $Q_\theta(s, a)$ to be a graph neural network (GNN). Our graph encoding of (G, V) has three main kinds of vertices: (i) objects o in G, (ii) relationships $\rho \in \mathcal{R}$, and (iii) variables $z \in \mathcal{Z}$, as well as a few auxiliary kinds of vertices to support the graph encoding. In Figure 2, we show an example of a graph encoding of a state in our MDP.

First, each object o is represented by exactly one vertex in the graph; each relationship $\rho \in \mathcal{R}$ is represented by exactly one vertex in the graph; and each variable $z \in \mathcal{Z}$ is represented by exactly one vertex in the graph.

Second, for each relationship $\rho_i(o_{i,1}, ..., o_{i,n_i}) \in G$, we introduce $n + 1$ new vertices $\{(i, \rho_i), (i, 1), ..., (i, n_i)\}$ into the graph, along with the edges

$$(i, \rho_i) \to (i, 1) \to o_1, ..., (i, \rho_i) \to (i, n_i) \to o_{n_i}$$

as well as the edge $\rho_i \to (i, \rho_i)$. This approach serves two purposes. The first purpose is that the intermediate vertex (i, ρ_i) distinguishes different relationships in G with the same type $\rho_i \in \mathcal{R}$. In addition, the edges $\rho_i \to (i, \rho_i)$ connects all relationship of the same type, which allows information to flow between these parts of the graph—for example, these edges could help the GNN count how many occurrences of the relationship "red" are in G. The second purpose is that the intermediate vertices (i, j) preserve information about the ordering of the objects in the relationship—e.g., in front(o, o'), the edge $(i, 0) \to o$ indicates that o is in front, and $(i, 1) \to o'$ indicates that o' is behind.

Third, to encode the valuations $v \in V$, we include the following edges in the graph:

$$\bigcup_{v \in V} \{z \to v(z) \mid z \in \mathcal{Z}\}.$$

Intuitively, these edges capture all possible assignments of objects o to variables z that are allowed by V. For instance, in the initial state $S_0 = (G, \mathcal{V})$, these edges are $z \to o$ for every $z \in \mathcal{Z}$ and o in G. This encoding loses information about V, since an assignment o to z may only be allowed for a subset of $v \in V$. However, V is combinatorial in size, so encoding the entire structure of V yields too large a graph.

To ensure that information can flow both ways, all edges in our encoding described above are bidirectional.

Finally, for settings $G = (G_+, G_?)$ where we consider uncertain relationships, we encode whether the relationship is certain as an edge type $\rho \xrightarrow{+} (i, \rho_i)$ for certain relationships in G_+ and $\rho \xrightarrow{?} (i, \rho_i)$ for uncertain relationships in $G_?$. Similarly, we use $z \xrightarrow{+} v(z)$ for certain valuations $v \in V_+$ and $z \xrightarrow{?} v(z)$ for uncertain valuations $v \in V_?$.

Neural network architecture. As mentioned above, $Q_\theta(s, a)$ is based on a graph convolutional network (GCN) (Kipf & Welling, 2017). We use $\psi(s)$ to denote the graph encoding of $s = (G, V)$ described above, where in addition each node is represented by a fixed embedding vector depending on its node name. The relationship vertices ρ and (i, ρ_i) have an embedding vector x_ρ. The positional vertices (i, j) encoding object ordering use an single embedding $x_{\rho_i, j}$ specific to both the corresponding relationship ρ_i and the object position j within the relationship.

Now, Q_θ applies a sequence of graph convolutions to $\psi(s)$:

$$\psi^{(0)} = \psi(s)$$
$$\psi^{(t+1)} = f_\theta^{(t)}(\psi^{(t)}) \quad (\forall t \in \{0, 1, ..., m-1\}.$$

Each $\psi^{(t)}$ has the same graph structure as $\psi(s)$, but the embedding vectors $x_k^{(t)}$ associated with each vertex k are different (i.e., computed as a function of the embeddings in the previous layer and of the GCN parameters).

Finally, at the output layer, Q_θ decodes the Q-values for each action $\rho(z_1, ..., z_n)$ based on the embedding vectors of the corresponding vertices $\rho, z_1, ..., z_n$:

$$Q_\theta(s, \rho(z_1, ..., z_n)) = g_\theta(x_\rho^{(m)}, x_{z_1}^{(m)}, ..., x_{z_n}^{(m)})$$

The architecture of g_θ can be any aggregation method from vertex level to action level. Two example strategies are LSTM structure and concatenation.

Hierarchical synthesis. We adopt an approach based on *hierarchical synthesis* (Nye et al., 2019). The idea is to combine a neurosymbolic synthesizer with a traditional one based on enumerative search. Intuitively, the neurosymbolic synthesizer can determine the majority of the program, after which the enumerative synthesizer can be used to complete the program into one that satisfies $\phi_G(P)$.

More precisely, in the first phase, we run the neurosymbolic synthesizer for a fixed number N of steps. At each step in this phase, we generate a program P of length M; if we find one that satisfies $\phi_G(P)$, then we return it. Otherwise, we continue to the second phase. In this phase, we begin by constructing the best program P^0 of length $M - K$ according to Q_θ (i.e., use zero exploration $\epsilon = 0$), where $K \in \mathbb{N}$ is a hyperparameter of our algorithm. Then, we perform an exhaustive search over programs P of length K, checking if the combined program $P' = P^0 \wedge P$ satisfies $\phi_G(P')$. If we find such a program, then we return it. Finally, we return $\varnothing$ if we do not find a valid program, indicating failure.

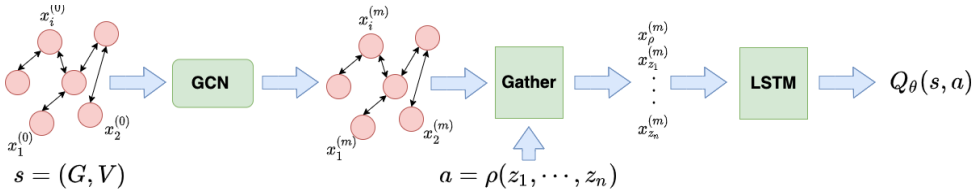

Figure 4. Our Q-network architecture. It takes as input an encoding of the state as a graph, and produces a vector embedding for each node using a GCN. Then, it predicts $Q(s, a)$ based on the vector embeddings for the nodes in the graph relevant to the action a.

Meta-learning. Finally, the algorithm we have described so far is for synthesizing a single referring relational program from scratch for a given scene graph G. We use a simple meta-learning approach where we pretrain Q_θ on a training benchmark of similar synthesis problems. In particular, we assume given a training set $\mathcal{G}_{\text{train}} \subseteq \mathcal{G}$ of scene graphs; then, we use deep Q-learning to train a neural network Q_{θ^0} that achieves high reward on average for random

$$\theta^0 = \arg\max_\theta \mathop{\mathbb{E}}_{G \sim \text{Uniform}(\mathcal{G}_{\text{train}})} [J(\theta; G)],$$

where $J(\theta; G)$ is the standard Q-learning objective for the MDP constructed for scene graph G.

Overall algorithm. Our overall algorithm is summarized in Algorithm 1. It takes as input a scene graph G, and outputs a relational referring program P (i.e., that satisfies $\phi_G(P)$), or $\varnothing$ if it fails to find such a program. The first step initializes Q_θ with the pretrained parameters θ^0. Then, the first phase uses deep Q-learning to tune θ based on programs P of length M sampled from the MDP for G. If no valid program is found, then it proceeds to the second phase, where it performs an exhaustive enumerative search over programs $P^0 \wedge P$, where P^0 is the optimal program of length $M - K$ according to Q_θ. If again no valid program is found, then it returns $\varnothing$ to indicate failure.

4. Experiments

We evaluate our approach on the CLEVR dataset, both (i) on purely synthetic graphs that we generated, and (ii) on graphs constructed using a CNN based on the synthetic images in the dataset. As we discuss below, we focus on synthetic data since it allows us to generate challenging problem instances that require the use of relationships involving multiple objects (in this case, spatial relationships). We show that our approach outperforms several baselines on these datasets.

4.1. Experimental Setup

Synthetic graphs. The first dataset is a set of synthetic scene graphs that include objects and relations between these objects, including unary ones (called *attributes*), namely shape, color, and material, as well as binary ones that encode spatial relations, namely front/behind and left/right. Using this approach, we can create challenging problem instances (i.e., a scene graph and a target object) to evaluate our algorithm. Our primary goal is to create problem instances where the referring relational program has to include spatial relationships to identify the target object. These instances are challenging since multiple relations are needed to distinguish two identical objects—e.g., in Figure 1 (left), at least two relations are needed to distinguish G from H, and more are needed in Figure 1 (right).

To this end, we create graphs with multiple identical objects in the scene. We classify these datasets by the set of counts of identical objects (in terms of attributes). For instance, the dataset CLEVR-4-3 consists of 7 objects total, the first 4 and last 3 of which have identical attributes—e.g., it might contain 4 gray metal cubes and 3 red metal spheres.

For simplicity, we directly generate scene graphs; thus, they do not contain any uncertainty. We impose constraints on the graphs to ensure they can be rendered into actual CLEVR images if desired. We consider the following datasets: 3-1-1-1-1, 4-1-1-1-1, 5-1-1-1, 6-1, 5-2, and 4-3. For each dataset, we use 7 total objects. Each dataset has 30 scene graphs for training (a total of 210 problem instances), and 500 scene graphs for testing (a total of 3500 problem instances).

CLEVR images. We also evaluate based on a dataset of images from the original CEVR dataset. These images have the same kinds of relations as our generated scene graphs.

We use a convolutional neural network (CNN) to construct the scene graph (Yi et al., 2018). For simplicity, this CNN predicts both object attributes and positions. The object attributes are predicted independently—i.e., it could predict that object J is both red with probability 0.75 and purple with probability 0.75. We consider a relation to be absent if $p = p(\rho(o_1, ..., o_n)) < 1/2$; for relations with $p \geq 1/2$, we consider them to be uncertain if there are multiple such attributes of the type (e.g., object J is predicted to be both red and purple with probability $\geq 1/2$), and certain otherwise. The spatial relationships are inferred based on the object positions; we consider it to be uncertain if the objects are very close together along some dimension.

Our algorithm. We search for programs of length at most $M = 8$, using $K = 2$ in hierarchical synthesis. We consider

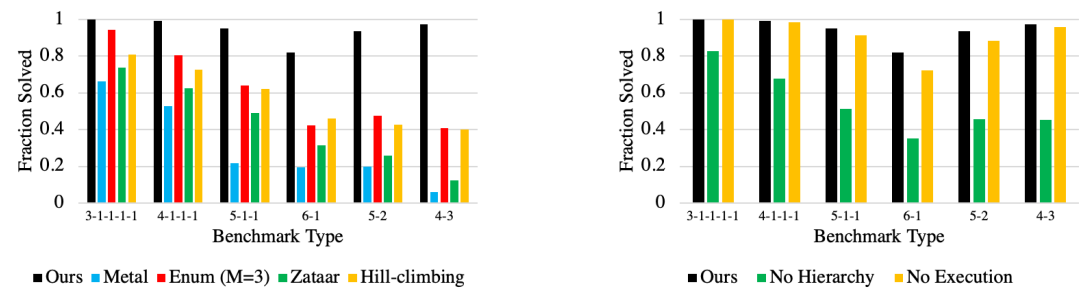

Figure 5. Fraction of problem instances solved in our benchmarks. Left: Comparing our algorithm (black) to baselines neurosymbolic synthesis (blue), enumerative synthesis with $M = 3$ (red), SMT-based synthesis (green), and hill-climbing synthesis (yellow). Right: Comparing our algorithm (black) to ablations without hierarchical synthesis (green) and without execution guidance (yellow).

three variables—i.e., $|\mathcal{Z}| = 3$, including z_t. We use $N = 200$ rollouts during reinforcement learning. We pretrain our Q-network on the training set corresponding to each dataset, using $N = 10000$ gradient steps with a batch size of 5.

4.2. Comparison to Baselines

We use each algorithm on our synthetic graphs dataset; in Figure 5 (left), we report what fraction of each kind of problem instance that is solved by each one.

Neurosymbolic synthesis. We compare to a state-of-the-art synthesizer called Metal (Si et al., 2018b). This approach uses reinforcement learning to find a program that satisfies the given specification; in addition, they use the same simple meta-learning approach as ours. As can be seen in Figure 5, our approach substantially outperforms this baseline by using hierarchical synthesis and execution-guided synthesis. For instance, on 6-1, our approach solves 82%; in contrast, Metal solves just 19%. Similarly, on 4-3, our approach solves 97% whereas Metal solves just 6%. We believe Metal works poorly in our setting due to the lack of intermediate feedback in our setting.

Enumerative synthesis. We compare to a synthesis algorithm that enumerates programs to find one that solves the task (Alur et al., 2013). This approach does not use machine learning to guide its search, making it challenging to scale to large programs (i.e., large M) due to the combinatorial blowup in the search space; thus, we consider $M = 3$. As can be seen in Figure 5, our approach substantially outperforms enumerative synthesis. For instance, on 6-1, our approach solves 82%, whereas enumerative synthesis solves 42%, and on 4-3, our approach solves 97%, whereas enumerative synthesis solves 41%.

SMT-based synthesis. There have been a number of recent tools for synthesizing Datalog programs using SMT solvers. However, these approaches typically perform best when the solutions are sparse in the search space, enabling the solvers to quickly prune large parts of the search space. In our setting, solutions are sufficiently common that pruning the search space is difficult. To demonstrate this gap, we have compared to a state-of-the-art Datalog synthesizer called Zaatar (Albarghouthi et al., 2017) based on the Z3 SMT solver (De Moura & Bjørner, 2008). As can be seen in Figure 5, our approach substantially outperforms Zataar. For instance, on 6-1, our approach solves 82%, whereas Zaatar solves 31%. Similarly, on 4-3, our approach solves 97%, whereas Zataar solves 12%. We also considered Prosynth (Raghothaman et al., 2019), a recent Datalog synthesizer based on CEGIS. However, Prosynth is designed for synthesizing programs with multiple smaller Datalog rules rather than synthesizing a single long Datalog rule, and did not terminate in 10 minutes on any of our benchmarks.

Hill-climbing synthesis. We compare to a Datalog synthesis algorithm that selects the clauses using hill-climbing (De Raedt & Kersting, 2003). At each step, this approach greedily selects the next clause to be the one that eliminates the most bindings for the target variable. As can be seen in the Figure 5, our approach substantially outperforms the hill-climbing synthesizer. For instance, on 6-1, our approach solves 82%, whereas the hill-climbing synthesizer solves 46%, and on 4-3, our approach solves 97%, whereas the hill-climbing synthesizer solves 40%.

4.3. Comparison to Ablations

We compare to two ablations on the synthetic graph datasets; in Figure 5 (right), we report what fraction of the benchmarks in each category are solved.

Hierarchical synthesis. Next, we compare to an ablation that does not use hierarchical synthesis—i.e., it only count the program generated by the neural symbolic synthesizer, but no enumerative search to correct the generated program. As can be seen, our approach substantially outperforms this ablation—e.g., on 6-1, hierarchical synthesis improves performance from 35% to 82%, and on 4-3, it improves performance from 46% to 97%. Intuitively, hierarchical synthesis improves performance by using reinforcement learning to find the larger but more straightforward parts of

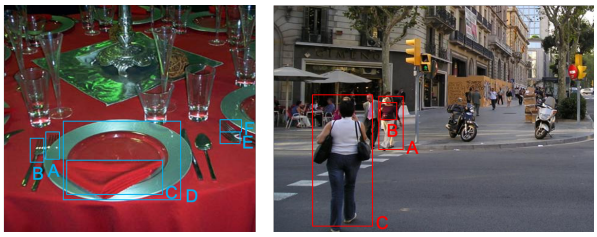

Program:

```
large(var0)
/\ left(var0, var1)
```

Output:

{var0 = A, var1 = C}
{var0 = A, var1 = D}
{var0 = A, var1 = E}
{var0 = A, var1 = F}

Program:

```
wearing(var0, var1)
/\ color(var1, red)
```

Output:

{var0 = A, var1 = B}

Figure 6. Examples from the GQA dataset (Hudson & Manning, 2019). We show bounding boxes for objects relevant to the query. In both cases, the target object is object A. We show the program synthesized using our approach based on the ground truth scene graphs, along with the possible variable bindings.

the program, whereas the enumerative synthesizer can find the more challenging parts using brute force.

Execution guidance. We compare to an ablation where we do not use the interpreter to guide RL; instead, the states are partial programs P. In particular, this ablation does not have feedback from the interpreter until the sparse reward at the very end of a rollout. As can be seen from Figure 5, using execution guidance improves our performance, especially on harder benchmarks—e.g., for the 6-1 benchmark, it improves performance from 72% to 82%.

4.4. CLEVR Images

We tested our approach on CLEVR images where we constructed the scene graph using a CNN (Yi et al., 2018). Out of 6487 tasks, our approach solved all but 25 according to the ground truth relations—i.e., the ground truth in the CLEVR dataset, not the predicted ones seen by our interpreter. Thus, our approach works well even when there is uncertainty in the scene graph predicted using a CNN. We compared to an ablation that ignores the uncertainty in the predicted scene graph; it correctly solves all but 79 of the 6487 tasks, which is more than 3× the failure rate.

5. Discussion

We have focused on generating programmatic referring expressions on the synthetic CLEVR dataset. There are two gaps compared to the original task (Golland et al., 2010; Kazemzadeh et al., 2014): (i) the original goal is to generate a natural language expression, and (ii) the original goal is to do so for real-world images. We discuss in detail below.

Natural language expressions. While we have focused on generating programmatic expressions since we can reason about their semantics, we have implemented an approach for translating a program P to natural language. First, we select a single valuation $v \in [\![P]\!]_G$ of the variables to construct the translation; intuitively, we observe that natural language expressions tend to try and bind each "variable" to a unique object, whereas our programs can have multiple bindings (e.g., program 2 in Figure 1). Second, we associate each variable z_i in P with the identifying phrase "object i", except the target object, which is associated with "target object". Third, for each z_i, we add a sentence indicating the unary attributes of object $v(z_i)$ according to P; in addition, we always include the shape and color of $v(z_i)$. Fourth, for each binary relation in P, we include a sentence indicating that relation. For example, the natural language referring expression generated based on program 1 in Figure 1 is:

> Object 1 is a brown sphere.
>
> The target object is a gray cube.
>
> The target object is in front of object 1.

While this approach produces expressions that are clear to humans, they are highly structured and do not capture the variety of human-generated expressions.

Real-world images. We focus on CLEVR both because it allows us to generate challenging benchmarks, and because predicting scene graphs for real-world images remains a challenging problem, though there has been recent progress (Krishna et al., 2017; Xu et al., 2017; Zellers et al., 2018). To illustrate the challenges, we generated referring expressions based on the ground truth scene graphs from the GQA dataset (Hudson & Manning, 2019). There are two challenges we encountered: (i) many objects and relationships are not labeled in the ground truth, and (ii) the target object is often trivial to identify. Nevertheless, we show two of the successful examples in Figure 6. On the left, the goal is to identify the fork labeled A, which must be distinguished from the other forks labeled B, E, and F. The generated program roughly translates to "the large fork to the left of the object", where the "object" can be the napkin labeled C, the plate labeled D, or one of the two other forks labeled E and F. On the right, the goal is to identify the woman labeled A, which must be distinguished from the other woman labeled C. The generated program roughly translates to "the woman wearing the red shirt".

6. Conclusion

We have proposed an approach to solving a symbolic variant of referring expressions using program synthesis. Our work is a first step towards incorporating symbolic reasoning into image captioning tasks. Future work includes translating our programs into natural language in a way that is both clear and "natural" (i.e., more similar to natural language), and applying our approach to real-world images.

Acknowledgements

We thank the anonymous reviewers for insightful comments. This research was supported in part by NSF awards #1836936, #1836822, #1652140, and CCF-1910769, and ONR award #N00014-18-1-2021.

References

Albarghouthi, A., Koutris, P., Naik, M., and Smith, C. Constraint-based synthesis of datalog programs. In *International Conference on Principles and Practice of Constraint Programming*, pp. 689–706. Springer, 2017.

Alur, R., Bodik, R., Juniwal, G., Martin, M. M., Raghothaman, M., Seshia, S. A., Singh, R., Solar-Lezama, A., Torlak, E., and Udupa, A. *Syntax-guided synthesis*. IEEE, 2013.

Balog, M., Gaunt, A. L., Brockschmidt, M., Nowozin, S., and Tarlow, D. Deepcoder: Learning to write programs. In *ICLR*, 2017.

Bastani, O., Pu, Y., and Solar-Lezama, A. Verifiable reinforcement learning via policy extraction. In *NIPS*, 2018.

Bunel, R., Hausknecht, M., Devlin, J., Singh, R., and Kohli, P. Leveraging grammar and reinforcement learning for neural program synthesis. In *ICLR*, 2018.

Chen, X., Liu, C., and Song, D. Execution-guided neural program synthesis. In *ICLR*, 2018.

Cohen, W. W., Yang, F., and Mazaitis, K. R. Tensorlog: Deep learning meets probabilistic databases. *Journal of Artificial Intelligence Research*, 1:1–15, 2018.

De Moura, L. and Bjørner, N. Z3: An efficient smt solver. In *International conference on Tools and Algorithms for the Construction and Analysis of Systems*, pp. 337–340. Springer, 2008.

De Raedt, L. and Kersting, K. Probabilistic logic learning. *ACM SIGKDD Explorations Newsletter*, 5(1):31–48, 2003.

De Raedt, L., Kimmig, A., and Toivonen, H. Problog: A probabilistic prolog and its application in link discovery. In *IJCAI*, volume 7, pp. 2462–2467. Hyderabad, 2007.

Dong, H., Mao, J., Lin, T., Wang, C., Li, L., and Zhou, D. Neural logic machines. In *ICLR*, 2019.

Ellis, K., Solar-Lezama, A., and Tenenbaum, J. Unsupervised learning by program synthesis. In *Advances in neural information processing systems*, pp. 973–981, 2015.

Ellis, K., Morales, L., Meyer, M. S., Solar-Lezama, A., and Tenenbaum, J. B. Dreamcoder: Bootstrapping domain-specific languages for neurally-guided bayesian program learning. In *NeurIPS*, 2018a.

Ellis, K., Ritchie, D., Solar-Lezama, A., and Tenenbaum, J. Learning to infer graphics programs from hand-drawn images. In *Advances in Neural Information Processing Systems*, pp. 6060–6069, 2018b.

Feng, Y., Martins, R., Bastani, O., and Dillig, I. Program synthesis using conflict-driven learning. In *PLDI*, pp. 420–435, 2018.

Gaunt, A. L., Brockschmidt, M., Kushman, N., and Tarlow, D. Differentiable programs with neural libraries. In *Proceedings of the 34th International Conference on Machine Learning-Volume 70*, pp. 1213–1222. JMLR. org, 2017.

Golland, D., Liang, P., and Klein, D. A game-theoretic approach to generating spatial descriptions. In *Proceedings of the 2010 conference on empirical methods in natural language processing*, pp. 410–419. Association for Computational Linguistics, 2010.

Hudson, D. A. and Manning, C. D. Gqa: A new dataset for real-world visual reasoning and compositional question answering. In *Proceedings of the IEEE Conference on Computer Vision and Pattern Recognition*, pp. 6700–6709, 2019.

Inala, J., Bastani, O., Tavares, Z., and Solar-Lezama, A. Synthesizing programmatic policies that inductively generalize. In *ICLR*, 2020.

Johnson, J., Hariharan, B., van der Maaten, L., Fei-Fei, L., Lawrence Zitnick, C., and Girshick, R. Clevr: A diagnostic dataset for compositional language and elementary visual reasoning. In *Proceedings of the IEEE Conference on Computer Vision and Pattern Recognition*, pp. 2901–2910, 2017.

Jothimurugan, K., Alur, R., and Bastani, O. A composable specification language for reinforcement learning tasks. In *Advances in Neural Information Processing Systems*, pp. 13021–13030, 2019.

Kazemzadeh, S., Ordonez, V., Matten, M., and Berg, T. Referitgame: Referring to objects in photographs of natural scenes. In *Proceedings of the 2014 conference on empirical methods in natural language processing (EMNLP)*, pp. 787–798, 2014.

Kipf, T. N. and Welling, M. Semi-supervised classification with graph convolutional networks. In *ICLR*, 2017.

Krishna, R., Zhu, Y., Groth, O., Johnson, J., Hata, K., Kravitz, J., Chen, S., Kalantidis, Y., Li, L.-J., Shamma, D. A., et al. Visual genome: Connecting language and vision using crowdsourced dense image annotations. *International Journal of Computer Vision*, 123(1):32–73, 2017.

Lake, B. M., Salakhutdinov, R., and Tenenbaum, J. B. Human-level concept learning through probabilistic program induction. *Science*, 350(6266):1332–1338, 2015.

Liu, R., Liu, C., Bai, Y., and Yuille, A. L. Clevr-ref+: Diagnosing visual reasoning with referring expressions. In *Proceedings of the IEEE Conference on Computer Vision and Pattern Recognition*, pp. 4185–4194, 2019.

Luo, R. and Shakhnarovich, G. Comprehension-guided referring expressions. In *Proceedings of the IEEE Conference on Computer Vision and Pattern Recognition*, pp. 7102–7111, 2017.

Ma, K., Francis, J., Lu, Q., Nyberg, E., and Oltramari, A. Towards generalizable neuro-symbolic systems for commonsense question answering. *arXiv preprint arXiv:1910.14087*, 2019.

Manhaeve, R., Dumancic, S., Kimmig, A., Demeester, T., and De Raedt, L. Deepproblog: Neural probabilistic logic programming. In *Advances in Neural Information Processing Systems*, pp. 3749–3759, 2018.

Mao, J., Gan, C., Kohli, P., Tenenbaum, J. B., and Wu, J. The neuro-symbolic concept learner: Interpreting scenes, words, and sentences from natural supervision. In *ICLR*, 2019.

Menon, A., Tamuz, O., Gulwani, S., Lampson, B., and Kalai, A. A machine learning framework for programming by example. In *ICML*, pp. 187–195. Proceedings of Machine Learning Research, 2013.

Nye, M., Hewitt, L., Tenenbaum, J., and Solar-Lezama, A. Learning to infer program sketches. In *ICML*, 2019.

Parisotto, E., Mohamed, A.-r., Singh, R., Li, L., Zhou, D., and Kohli, P. Neuro-symbolic program synthesis. In *ICLR*, 2017.

Pu, Y., Miranda, Z., Solar-Lezama, A., and Kaelbling, L. Selecting representative examples for program synthesis. In *International Conference on Machine Learning*, pp. 4158–4167, 2018.

Raghothaman, M., Mendelson, J., Zhao, D., Naik, M., and Scholz, B. Provenance-guided synthesis of datalog programs. *Proceedings of the ACM on Programming Languages*, 4(POPL):1–27, 2019.

Redmon, J., Divvala, S., Girshick, R., and Farhadi, A. You only look once: Unified, real-time object detection. In *Proceedings of the IEEE conference on computer vision and pattern recognition*, pp. 779–788, 2016.

Santoro, A., Raposo, D., Barrett, D. G., Malinowski, M., Pascanu, R., Battaglia, P., and Lillicrap, T. A simple neural network module for relational reasoning. In *Advances in neural information processing systems*, pp. 4967–4976, 2017.

Santoro, A., Faulkner, R., Raposo, D., Rae, J., Chrzanowski, M., Weber, T., Wierstra, D., Vinyals, O., Pascanu, R., and Lillicrap, T. Relational recurrent neural networks. In *Advances in neural information processing systems*, pp. 7299–7310, 2018.

Si, X., Lee, W., Zhang, R., Albarghouthi, A., Koutris, P., and Naik, M. Syntax-guided synthesis of datalog programs. In *Proceedings of the 2018 26th ACM Joint Meeting on European Software Engineering Conference and Symposium on the Foundations of Software Engineering*, pp. 515–527, 2018a.

Si, X., Yang, Y., Dai, H., Naik, M., and Song, L. Learning a meta-solver for syntax-guided program synthesis. In *ICLR*, 2018b.

Si, X., Raghothaman, M., Heo, K., and Naik, M. Synthesizing datalog programs using numerical relaxation. In *IJCAI*, 2019.

Valkov, L., Chaudhari, D., Srivastava, A., Sutton, C., and Chaudhuri, S. Houdini: Lifelong learning as program synthesis. In *Advances in Neural Information Processing Systems*, pp. 8701–8712, 2018.

Verma, A., Murali, V., Singh, R., Kohli, P., and Chaudhuri, S. Programmatically interpretable reinforcement learning. In *ICML*, 2018.

Verma, A., Le, H., Yue, Y., and Chaudhuri, S. Imitation-projected programmatic reinforcement learning. In *Advances in Neural Information Processing Systems*, pp. 15726–15737, 2019.

Wang, P.-W., Donti, P. L., Wilder, B., and Kolter, Z. Satnet: Bridging deep learning and logical reasoning using a differentiable satisfiability solver. *arXiv preprint arXiv:1905.12149*, 2019.

Xu, D., Zhu, Y., Choy, C. B., and Fei-Fei, L. Scene graph generation by iterative message passing. In *CVPR*, pp. 5410–5419, 2017.

Yi, K., Wu, J., Gan, C., Torralba, A., Kohli, P., and Tenenbaum, J. Neural-symbolic vqa: Disentangling reasoning from vision and language understanding. In *Advances in*

Neural Information Processing Systems, pp. 1031–1042, 2018.

Young, H., Bastani, O., and Naik, M. Learning neurosymbolic generative models via program synthesis. In *ICML*, 2019.

Yu, L., Poirson, P., Yang, S., Berg, A. C., and Berg, T. L. Modeling context in referring expressions. In *European Conference on Computer Vision*, pp. 69–85. Springer, 2016.

Yu, L., Tan, H., Bansal, M., and Berg, T. L. A joint speaker-listener-reinforcer model for referring expressions. In *Proceedings of the IEEE Conference on Computer Vision and Pattern Recognition*, pp. 7282–7290, 2017.

Zellers, R., Yatskar, M., Thomson, S., and Choi, Y. Neural motifs: Scene graph parsing with global context. In *CVPR*, pp. 5831–5840, 2018.